Unified Bit-Based Probabilistic Data Association Aided MIMO Detection for High-Order QAM Constellations

Shaoshi Yang, *Student Member, IEEE*, Tiejun Lv, *Member, IEEE*, Robert G. Maunder, *Member, IEEE*, and Lajos Hanzo, *Fellow, IEEE*

***Abstract*—A unified bit-based probabilistic data association (B-PDA) detection approach is proposed for multiple-input–multiple-output (MIMO) systems employing high-order rectangular quadrature amplitude modulation (QAM). The new approach transforms the symbol detection process of QAM to a bit-based process by introducing a unified matrix representation (UMR) of QAM. Both linear natural and nonlinear binary reflected Gray bit-to-symbol mappings are considered. With the aid of simulation results, we demonstrate that the linear-natural-mapping-based B-PDA approach typically attained an improved detection performance [measured in terms of both bit error ratio (BER) and symbol error ratio (SER)] in comparison with the conventional symbol-based probabilistic data association (PDA)-aided MIMO detector, despite its dramatically reduced computational complexity. The only exception is that, at low SNRs, the linear-natural-mapping-based B-PDA is slightly inferior in terms of its BER to the conventional symbol-based PDA using binary reflected Gray mapping. Furthermore, the simulation results show that the linear-natural-mapping-based B-PDA MIMO detector may approach the best-case performance provided by the nonlinear binary reflected Gray-mapping-based B-PDA MIMO detector under ideal conditions. Additionally, the implementation of the B-PDA MIMO detector is shown to be much simpler in the case of the linear natural mapping. Based on these two points, we conclude that, in the context of the uncoded B-PDA MIMO detector, it is preferable to use the linear natural bit-to-symbol mapping, rather than the nonlinear Gray mapping.**

***Index Terms*—High-order quadrature amplitude modulation (QAM), low complexity, probabilistic data association (PDA), unified matrix representation (UMR), vector detection.**

I. Introduction

THE SUBSTANTIAL spectral efficiency gains promised by multiple-input–multiple-output (MIMO) [1] techniques have stimulated substantial research activities, particularly as far as their detection is concerned. The optimum maximum-likelihood (ML) detector [2] exhibits an exponentially increasing complexity upon increasing the number of jointly detected symbols, which generally precludes its application in practical MIMO systems. The ML detector can also be implemented using more efficient[1] algorithms, such as sphere decoding (SD) [3]. However, SD cannot always efficiently limit the complexity of high-dimensional problems associated with a large number of transmit antennas or high-order modulation (HOM), particularly when aiming for using soft decisions at low SNRs [4]. There are dozens of other suboptimal MIMO detectors ranging from the most common zero forcing (ZF), minimum mean square error (MMSE), and successive interference cancellation (SIC) to expectation maximization (EM) and semidefinite relaxation (SDR), etc. (See [5]–[9] and the references within.) However, they either have a modest performance (ZF, MMSE, and SIC) or might have a computational complexity that is exponential in the number of sources (EM) [7] or impose considerably increased computational complexity, which increases at a rate spanning from at least $O(N^{3.5})$ [9] to $O(K^{6.5}N^{6.5})$ [10] for high-order quadrature amplitude modulation (QAM), where $N = O(N_T)$, N_T is the size of the transmitted QAM symbol vector, and K is the square root of the constellation size (SDR). Since MIMO-aided HOM will play a pivotal role in next-generation wireless systems, there is a need to develop low-complexity MIMO detectors that are appropriate for HOM.

The probabilistic data association (PDA) method [11], which was originally conceived for target tracking [12], may also be developed into a reduced-complexity design alternative to maximum *a posteriori* (MAP) probability decoders/detectors/equalizers, which are known to constitute the optimal soft-decision approach. Hence, the PDA algorithm constitutes a promising detection technique. First, it may achieve a near-optimal detection performance, particularly in the context of code-division multiple-access (CDMA) systems [11], [13]. Second, it has a low complexity that increases no faster than $O(L^3)$, where L is either the number of users in CDMA [11] or the number of transmit antennas in the MIMO system [17]. Third, it is inherently a soft-input–soft-output (SISO) algorithm, which is eminently applicable in combination with

Manuscript received April 26, 2010; revised September 12, 2010 and December 17, 2010; accepted January 30, 2011. Date of publication February 14, 2011; date of current version March 21, 2011. This work was supported in part by the National Natural Science Foundation of China under Grant NSFC-60972075, by the China Scholarship Council, and by the Engineering and Physical Sciences Research Council, U.K., and the European Union under the auspices of the OPTIMIX project. The review of this paper was coordinated by Prof. H. Liu.

S. Yang, R. G. Maunder, and L. Hanzo are with the School of Electronics and Computer Science, University of Southampton, SO17 1BJ Southampton, U.K. (e-mail: sy7g09@ecs.soton.ac.uk; rm@ecs.soton.ac.uk; lh@ecs.soton.ac.uk).

T. Lv is with the Key Laboratory of Universal Wireless Communications, Beijing University of Posts and Telecommunications, Beijing 100876, China (e-mail: lvtiejun@bupt.edu.cn).

Digital Object Identifier 10.1109/TVT.2011.2114376

[1]This efficiency is quantified in terms of the average computational cost at reasonable signal-to-noise ratios (SNRs), as shown in [4].

forward error control (FEC) coding.[2] Furthermore, the higher the number of transmit antennas or users, the better its performance, provided that the channel is not rank deficient [14]. The PDA approach was recently extended to the symbol detection of MIMO systems [15]–[17], striking an excellent tradeoff between the attainable performance and the complexity imposed. The pseudocovariance [18] was employed to fully specify its complex Gaussian input distribution, and the resultant Complex-valued formulation of the PDA (CPDA) [17] was shown to outperform both the real-valued vector formulation of the Generalized PDA (GPDA) [15] and the Complex-valued PDA using an approximately matched mean and covariance (CPDA-apx) [16]. However, it may be readily shown that the performance versus complexity benefits of the conventional symbol-based PDA-aided MIMO detectors [15]–[17] are not as convincing as those of their CDMA-based counterpart [11]. According to the results in [14], one of the reasons is that the number of transmit antennas in a MIMO system is typically lower than that of the users in CDMA. A second reason is that, typically, QAM is used in MIMO systems, rather than BPSK. In addition, it is also because the equivalent "channel" matrix in CDMA systems is more likely to be well conditioned than the channel matrix of MIMO systems.[3] As argued in [11], a key feature of PDA is the repeated conversion of a multimodal Gaussian mixture probability to a single Gaussian distribution having a matched mean and covariance. Hence, the accuracy of the Gaussian approximation dominates the attainable performance. In fact, it has been demonstrated in [14] that the quality of the Gaussian approximation in PDA is the best for a large number of transmit antennas and a small number of modulation constellation points. Therefore, the symbol-based PDA-aided MIMO detectors' performance significantly degrades for high-order QAM, compared with that of the ML/MAP detector, whereas its complexity substantially increases, owing to the increased number of symbol probabilities to be computed.

The aim of this paper is to develop an *efficient* PDA-based MIMO detector for high-order rectangular QAM constellations. Inspired by the conclusions of [14], we intend to find a method that may *equivalently* increase the length of the effective transmitted signal vector and/or reduce the effective constellation size for PDA MIMO detectors.

The main contributions in this paper are given as follows.

1) We present an explicit unified matrix representation (UMR) of both linear natural mapping [8], [20] and nonlinear binary reflected Gray-mapping-based rectangular QAM employed in MIMO systems, including BPSK modulation as a special case.
2) Based on the UMR, we first propose a bit-based PDA (B-PDA) MIMO detector for high-order rectangular QAM. In contrast to the conventional symbol-based PDA MIMO detectors of [15]–[17], the B-PDA transforms the symbol-based QAM detection of MIMO systems to a BPSK-like binary scenario, thus eliminating symbol-based decisions, and directly operates at the bit level. While a similar mathematical representation of the linear-natural-mapping-based rectangular QAM was also used in the context of the SDR technique of [8] and in the multilevel bit-interleaved coded modulation scheme of [20], its extension to the nonlinear binary reflected Gray mapping and its application to improving the PDA-based MIMO detectors have not been suggested before.
3) We investigate the complexity of the proposed B-PDA MIMO detector both analytically and by simulations. It is demonstrated that the linear-natural-mapping-based B-PDA substantially reduces the computational complexity, compared with the conventional symbol-based PDA MIMO detector in uncoded VBLAST systems using high-order QAM.
4) In addition to a beneficial complexity reduction, the simulation results show that the linear-natural-mapping-based B-PDA has a slightly improved performance in comparison with the conventional symbol-based PDA. Furthermore, it approaches the lower bound performance provided by the binary reflected Gray-mapping-based B-PDA under the idealized perfect modulation matrix estimation assumption.
5) Considering the additional complexity and the potential performance degradation entailed by the modulation matrix estimation for binary reflected Gray-mapping-based B-PDA, we argue that the binary reflected Gray mapping is not the best choice of labeling scheme for B-PDA. In fact, it is preferable to use the simpler and more practicable linear natural mapping for the B-PDA detector in the context of the uncoded VBLAST system considered.

II. Problem Statement

Consider a spatial-multiplexing MIMO system using N_T transmit and N_R receive antennas. The received baseband signal at each symbol instant is given by

$$\mathbf{y} = \mathbf{H}\mathbf{s} + \mathbf{n} \tag{1}$$

where $\mathbf{H}$ is the $(N_R \times N_T)$-element complex channel matrix, $\mathbf{s}$ is the length-N_T vector of transmitted symbols from a modulation constellation $\mathcal{A} = \{a_1, a_2, \ldots, a_M\}$ with cardinality M, and $\mathbf{n}$ represents the length-N_R complex-valued circularly symmetric Gaussian noise vector with zero mean and a covariance matrix of $N_0\mathbf{I}$, where $\mathbf{I}$ is an $(N_R \times N_R)$-element identity matrix.

Assume that the components of the transmitted symbol vector $\mathbf{s}$ are obtained using the bit-to-symbol mapping function $s_j = \text{map}(\mathbf{d}_j),\ j = 1, 2, \ldots, N_T$, where $\mathbf{d}_j = [d_{j,1}, d_{j,2}, \ldots, d_{j,M_c}]^T \in \{+1, -1\}^{M_c}$ is the vector of data bits, and

[2]Note that, however, in this paper, we intend to focus our attention on the hard detection of uncoded transmissions using PDA. The in-depth investigation of the iterative decoding based on PDA is somewhat out of context in this paper, and it will be heeded in our future work.

[3]The equivalent "channel" matrix in CDMA systems is usually constituted by the convolution of the channel impulse response and the cross-correlation matrix of the well-designed spreading codes, which is typically well conditioned. However, in MIMO systems, it is possible that the channel matrix for some channel realizations becomes rather ill conditioned. According to the central limit theorem, having fewer independent random variables imposed by the ill-conditioned matrices may result in poor Gaussian approximations, the quality of which is the principal determining factor of the PDA-based detectors' performance.

$M_c = \log_2 M$ is the number of bits per M-QAM symbol. The vector of bits corresponding to $\mathbf{s}$ is denoted as $\mathbf{b}$, which satisfies $\mathbf{s} = \text{map}(\mathbf{b})$ and is formed by concatenating the N_T antennas' bits $\mathbf{d}_1, \mathbf{d}_2, \ldots, \mathbf{d}_{N_T}$, yielding $\mathbf{b} = [b_1, b_2, \ldots, b_k, \ldots, b_{M_c N_T}] = [\mathbf{d}_1^T, \mathbf{d}_2^T, \ldots, \mathbf{d}_{N_T}^T]^T \in \{+1, -1\}^{M_c N_T}$.

At the receiver, the task of the conventional symbol-based PDA MIMO detector is to seek a small bit error ratio (BER) or symbol error ratio (SER) by estimating the *a posteriori* symbol probabilities $P(s_j = a_m|\mathbf{y}) = P_m(s_j|\mathbf{y})$, without an exhaustive search in the space of all possible M-QAM MIMO symbol combinations. In this paper, our goal is to attain a high detection performance by estimating the *a posteriori* bit probabilities $P(d_{j,q} = \pm 1|\mathbf{y}), q = 1, 2, \ldots, M_c$.

III. Unified Matrix Representation of Quadrature Amplitude Modulation: Linear Natural Bit-to-Symbol Mapping

The conventional description of the bit-to-symbol mapping process of QAM is based on a lookup table method complying with the specific mapping rules [19]. To some extent, this method conceals the mathematical characteristics of a specific bit-to-symbol mapping process.

In MIMO systems employing rectangular QAM, the mapping from bits to symbols may be compactly and explicitly formulated by a unified matrix transformation [8], [20] to be derived here. Consider a QAM constellation symbol $a_m = x + iy \; \forall m \in \{1, 2, \ldots, M\}$, where x and y are taken from the real alphabets $\mathcal{A}_{\text{real}}$ and $\mathcal{A}_{\text{imag}}$, respectively. For simplicity, we assume that each transmit antenna uses the same modulation scheme of $\mathcal{A}_{\text{real}} = \mathcal{A}_{\text{imag}} = \bar{\mathcal{A}} = \{\alpha_1, \alpha_2, \ldots, \alpha_{\sqrt{M}}\}$ for square QAM, although our approach may be generalized to different alphabets for the real and imaginary parts. Let us now rewrite the bit-to-symbol mapping function $s_j = \text{map}(\mathbf{d}_j)$ defined in Section II as

$$s_j = s_j^{\Re} + i s_j^{\Im} = \text{map}\left(d_{j,1}^{\Re}, \ldots, d_{j,M_c/2}^{\Re}, d_{j,M_c/2+1}^{\Im}, \ldots, d_{j,M_c}^{\Im}\right) \tag{2}$$

where $\Re$ and $\Im$ indicate the real and imaginary parts of s_j, respectively, and $s_j^{\Re}, s_j^{\Im} \in \bar{\mathcal{A}}$.

Since square QAM constellations having symmetric real and imaginary parts are considered here, it is sufficient to consider the real part only in the following derivation of the matrix representation without any loss of generality.

Let us assume that the elements of $\bar{\mathcal{A}}$ are placed in ascending order for constructing the vector $\mathbf{a} = [\alpha_1, \alpha_2, \ldots, \alpha_{\sqrt{M}}]^T$ and denote the corresponding bit strings as the $(\sqrt{M} \times (M_c/2))$-element matrix $\mathbf{B}$, in which the kth row is the bit string corresponding to α_k, $k = 1, 2, \ldots, \sqrt{M}$. Then, the bit-to-symbol mapping rule is described as

$$\mathbf{B}\mathbf{x} = \mathbf{a} \tag{3}$$

where we would like to express $\mathbf{x}$, i.e., the "subgenerating unit," which maps the bits to the real part of a QAM symbol. Furthermore, the vector $\mathbf{g} = [\mathbf{x}^T, i\mathbf{x}^T]$ is defined as the "generating unit" of the M-QAM, and it maps the bits to a QAM symbol.

Here, we consider the linear-natural-mapping-based square 64QAM as an example to elaborate on how to find the subgenerating unit $\mathbf{x}$. The alphabet $\bar{\mathcal{A}}$ of square 64QAM is given by $\mathcal{A}_{64\text{QAM}} = \{-7, -5, -3, -1, +1, +3, +5, +7\}$, $M_c = 6$, $\mathbf{B} = [-1, -1, -1; -1, -1, +1; -1, +1, -1; -1, +1, +1; +1, -1, -1; +1, -1, +1; +1, +1, -1; +1, +1, +1]$ (we use semicolon ";" to distinguish the different rows in $\mathbf{B}$), and $\mathbf{a} = [-7, -5, -3, -1, +1, +3, +5, +7]^T$; thus, we have $\mathbf{x} = [4, 2, 1]^T$ in the light of (3). The Hamming distances between neighboring constellation points in this case are either 1 or 2.

Similarly, we have $\mathbf{x} = [2, 1]^T$ for 16QAM and $\mathbf{x} = 1$ for 4QAM. It should be pointed out that the linear natural mapping presented here is the same as the binary reflected Gray mapping[4] for 4QAM. This observation will be beneficial for understanding the implications behind the matrix representation of Gray-mapping-based rectangular QAM in Section IV.

From the subgenerating units previously presented for 4QAM, 16QAM, and 64QAM, we can infer that, for general rectangular QAM, the UMR is given by

$$\mathbf{W} = \begin{pmatrix} \mathbf{g} & \cdots & \mathbf{0} \\ \vdots & \ddots & \vdots \\ \mathbf{0} & \cdots & \mathbf{g} \end{pmatrix}_{N_T \times M_c N_T} \tag{4}$$

where $\mathbf{g} = [2^{(M_c/2)-1}, 2^{(M_c/2)-2}, \ldots, 1, 2^{(M_c/2)-1} i, 2^{(M_c/2)-2} i, \ldots, i]$ for square QAM. While, for the odd rectangular QAM (8QAM, 32QAM, etc.), if we assume that the real alphabet of the odd rectangular QAM is the same as that of its double-sized square QAM counterpart, we obtain $\mathbf{g} = [2^{(M_c-1)/2}, 2^{((M_c-1)/2)-1}, \ldots, 1, 2^{((M_c-1)/2)-1} i, \ldots, i]$, including BPSK as a special case of a rectangular QAM signal, with its imaginary part being 0.

Consequently, the mapping function $\mathbf{s} = \text{map}(\mathbf{b})$ in Section II may be characterized by $\mathbf{s} = \mathbf{W}\mathbf{b}$ for MIMO systems using the linear-natural-mapping-based rectangular QAM.

IV. Unified Matrix Representation of Quadrature Amplitude Modulation: Nonlinear Gray Bit-to-Symbol Mapping

In Section III, we presented a UMR of general rectangular QAM constellations using linear natural mapping for MIMO systems. The limitation of this matrix representation is, however, that it did not provide the nonlinear Gray mapping for rectangular QAM constellations having cardinality larger than 4. (For 4QAM, the linear natural and the Gray bit-to-symbol mappings are identical.) Consequently, since the binary reflected Gray mapping was shown to be the optimal labeling scheme [21] in the sense of the lowest possible average probability of bit errors, two interesting questions arise: 1) Would the linear-natural-mapping-based B-PDA detector's performance degrade for high-order QAM, owing to the lack of Gray mapping in

[4]Although there may be distinct Gray labelings that result in different bit-error probabilities, particularly in high-order constellations, the binary reflected Gray mapping has been shown to give the lowest possible average probability of bit errors for conventional symbol-based detection under certain assumptions on the channel [21] We will simply use "Gray mapping" to refer to the "binary reflected Gray mapping" in the rest of the paper.

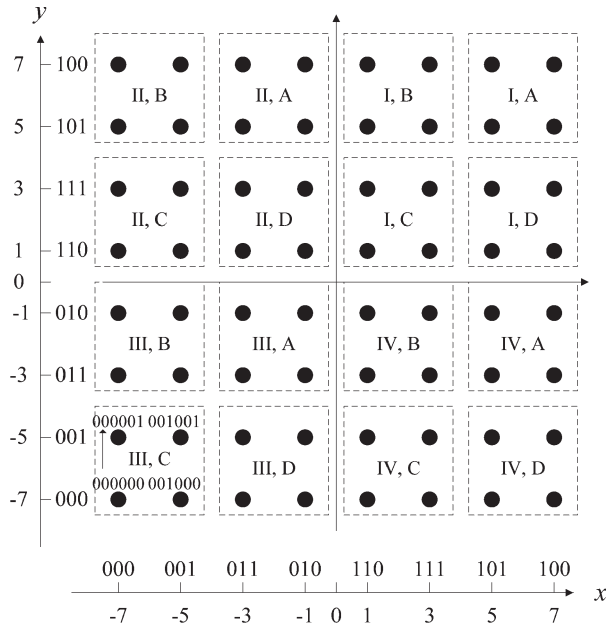

Fig. 1. Signal space diagram for 64QAM under Gray mapping.

the context of uncoded systems? 2) Is the Gray mapping still the best labeling scheme for the B-PDA MIMO detector? To answer these questions, in this section, we extend the previous linear-natural-mapping-based results to the nonlinear Gray mapping case. In contrast to the linear natural bit-to-symbol mapping scenario, the matrix representation of Gray mapping depends on the bits to be transmitted, as detailed here.

A. Example With 64QAM

According to (3) and the Gray mapping rule shown in Fig. 1, we have $\mathbf{a} = [-7, -5, -3, -1, +1, +3 + 5, +7]^T$, $\mathbf{x} = [a, b, c]^T$, and the original Gray-mapping-based bits 000, 001, 011, 010, 110, 111, 101, and 100 are converted into the bipolar representation of $\mathbf{B} = [-1, -1, -1; -1, -1, +1; -1, +1, +1; -1, +1, -1; +1, +1, -1; +1, +1, +1; +1, -1, +1; +1, -1, -1]$ under the rule of $2b_i - 1$, where b_i, $i = 1, 2$, is a binary digit of 0 or 1. Upon substituting $\mathbf{a}$, $\mathbf{B}$, and $\mathbf{x}$ into (3), we find that $\mathbf{x}$ does not have a unique solution, owing to the nonlinearity of Gray mapping. However, each of the following four subsystems of equations has a unique solution:

$$\begin{cases} \text{(i)} \begin{cases} -a-b-c=-7 \\ -a-b+c=-5 \end{cases} \Rightarrow [a,b,c]=[4,2,1] \\ \text{(ii)} \begin{cases} -a+b+c=-3 \\ -a+b-c=-1 \end{cases} \Rightarrow [a,b,c]=[4,2,-1] \end{cases} \tag{5}$$

$$\begin{cases} \text{(iii)} \begin{cases} a+b-c=1 \\ a+b+c=3 \end{cases} \Rightarrow [a,b,c]=[4,-2,1] \\ \text{(iv)} \begin{cases} a-b+c=5 \\ a-b-c=7 \end{cases} \Rightarrow [a,b,c]=[4,-2,-1]. \end{cases} \tag{6}$$

We can observe in (5) and (6) that there are four possible solution vectors, i.e., $\mathbf{x}_1 = [4, 2, 1]^T$, $\mathbf{x}_2 = [4, 2, -1]^T$, $\mathbf{x}_3 = [4, -2, 1]^T$, and $\mathbf{x}_4 = [4, -2, -1]^T$ corresponding to four 3-bit tuples (every three adjacent bits as a unit) in which $(-1, -1)$, $(-1, +1)$, $(+1, +1)$, and $(+1, -1)$ are the first two bits, respectively. Hence, for Gray mapping, the subgenerating unit has the aforementioned four legitimate values of (a, b, c). For example, if the 3-bit tuple to be transmitted is $(-1, -1, x)$, then its corresponding subgenerating unit is $(a = 4, b = 2, c = 1)$, and if the 3-bit tuple is $(+1, -1, x)$, then we have $(a = 4, b = -2, c = -1)$, where x is -1 or 1.

By jointly considering Fig. 1 and the subgenerating units of 64QAM previously derived, we may infer several pieces of useful information for 64QAM: 1) First, the component having the largest modulus in the generating unit remains the same as that of its counterpart in linear natural mapping, but the signs of the smaller components may change. 2) Second, the set of constellation points that dwell in the same four-point block within the dashed box of Fig. 1 share the same generating unit. Therefore, 64QAM is divided into 16 four-point blocks and has 16 different generating units constructed by four different subgenerating units. 3) Furthermore, the constellation points in the same half-plane are explicitly described by (5) (the left half-plane) and (6) (the right half-plane), each of which is composed by two further sets of equations, as seen in (i)–(iv) of (5) and (6), respectively. 4) Additionally, it is plausible that the solution of (a, b, c) for each of (i)–(iv) is unique under the constraint that (i) and (ii) constituting the left half-plane share the same values of (a, b), and so do (iii) and (iv), constituting the right half-plane.

B. General QAM

Based on the aforementioned insights drawn from 64QAM, the UMR of the most commonly used Gray mapping may be obtained by appropriately alternating the sign of certain entries in the preceding static UMR of the linear-natural-mapping-based QAM, which, in fact, serves as the basis matrix for Gray-mapping-aided QAM and may be prestored for memory-based access. The corresponding procedures are summarized as follows.

1) Generate the UMR of the linear natural bit mapping, i.e., $\mathbf{W}$ according to (4).
2) Check the sign of the bipolar bits in $\mathbf{b}$, and adjust the sign of the corresponding entries in $\mathbf{W}$ to get $\mathbf{W}(\mathbf{b})$ accordingly. The sign of the first element of the real and imaginary parts in $\mathbf{g}$ is always positive, whereas the signs of the remaining elements should be changed according to the various combinations of the residue bits. When taking into account the symmetry of the real and imaginary parts of the QAM constellation points and excluding the specific combination where each element is positive as in linear natural mapping, the number of additional different subgenerating units is $(2^{(M_c/2)-1} - 1)$ for the square QAM and $(2^{(M_c-1)/2} - 1)$ for the rectangular QAM representing an odd number of bits per symbol. The selection of the appropriate generating unit is illuminated using 16QAM and 64QAM as our examples in Table I. For ease of exposition, Matlab-style pseudocode is used. Based on the rules of Table I, the complete set of generating units of Gray-mapping-based 16QAM is presented in Table II as an example.

Therefore, the mapping function $\mathbf{s} = \text{map}(\mathbf{b})$ in Section II may be formulated as $\mathbf{s} = \mathbf{W}(\mathbf{b})\mathbf{b}$ for MIMO systems using the nonlinear Gray-mapping-based rectangular QAM.

TABLE I
UMR RULE OF GRAY MAPPING

16QAM ($M_c = 4$)	64QAM ($M_c = 6$)
for $k = 1{:}\frac{M_c}{2}{:}M_cN_T$ for $j = 1{:}N_T$ if $b_k == 1$ $\mathbf{W}(j, k+1) = -\mathbf{W}(j, k+1)$ end end end	for $k = 1{:}\frac{M_c}{2}{:}M_cN_T$ for $j = 1{:}N_T$ if $b_k == 1$ and $b_{k+1} == 1$ $\mathbf{W}(j, k+1) = -\mathbf{W}(j, k+1)$ elseif $b_k == -1$ && $b_{k+1} == 1$ $\mathbf{W}(j, k+2) = -\mathbf{W}(j, k+2)$ elseif $b_k == 1$ && $b_{k+1} == -1$ $\mathbf{W}(j, k+1) = -\mathbf{W}(j, k+1)$ $\mathbf{W}(j, k+2) = -\mathbf{W}(j, k+2)$ end end end

TABLE II
GENERATING UNITS OF 16QAM USING GRAY MAPPING

Index	Generating Unit	Bit Sequence	Symbol	Quadrant	Index	Generating Unit	Bit Sequence	Symbol	Quadrant
1	$2\ 1\ 2i\ i$	$-1\ -1\ -1\ -1$	$-3-3i$	III	9	$2\ -1\ 2i\ i$	$+1\ +1\ -1\ -1$	$1-3i$	IV
2	$2\ 1\ 2i\ i$	$-1\ -1\ -1\ +1$	$-3-i$		10	$2\ -1\ 2i\ i$	$+1\ +1\ -1\ +1$	$1-i$	
3	$2\ 1\ 2i\ -i$	$-1\ -1\ +1\ +1$	$-3+i$	II	11	$2\ -1\ 2i\ -i$	$+1\ +1\ +1\ +1$	$1+i$	I
4	$2\ 1\ 2i\ -i$	$-1\ -1\ +1\ -1$	$-3+3i$		12	$2\ -1\ 2i\ -i$	$+1\ +1\ +1\ -1$	$1+3i$	
5	$2\ 1\ 2i\ -i$	$-1\ +1\ +1\ -1$	$-1+3i$		13	$2\ -1\ 2i\ -i$	$+1\ -1\ +1\ -1$	$3+3i$	
6	$2\ 1\ 2i\ -i$	$-1\ +1\ +1\ +1$	$-1+i$		14	$2\ -1\ 2i\ -i$	$+1\ -1\ +1\ +1$	$3+i$	
7	$2\ 1\ 2i\ i$	$-1\ +1\ -1\ +1$	$-1-i$	III	15	$2\ -1\ 2i\ i$	$+1\ -1\ -1\ +1$	$3-i$	IV
8	$2\ 1\ 2i\ i$	$-1\ +1\ -1\ -1$	$-1-3i$		16	$2\ -1\ 2i\ i$	$+1\ -1\ -1\ -1$	$3-3i$	

V. BIT-BASED PROBABILISTIC DATA ASSOCIATION MULTIPLE-INPUT–MULTIPLE-OUTPUT DETECTION BASED ON UNIFIED MATRIX REPRESENTATION

We have provided a UMR of the rectangular M-QAM. Given the UMR, diverse MIMO signal processing problems involving high-order QAM may be simplified to a BPSK-like scenario. Here, we will further develop the conventional symbol-based PDA MIMO detector of [17] to a reduced-complexity bit-based approach.

A. Basic Detection Algorithm

Based on the UMR of QAM, we have $\mathbf{s} = \mathbf{W}\mathbf{b}$ and $\mathbf{s} = \mathbf{W}(\mathbf{b})\mathbf{b}$ for the linear natural mapping and nonlinear Gray mapping, respectively. We will first consider the linear-mapping-based rectangular QAM to elaborate on the B-PDA detector and then discuss the nonlinear Gray mapping scenario at the end of Section IV-B.

The original system model of (1) may be rewritten as

$$\mathbf{y} = \mathbf{H}\mathbf{W}\mathbf{b} + \mathbf{n} = \mathbf{Q}\mathbf{b} + \mathbf{n} \tag{7}$$

where $\mathbf{Q} = \mathbf{H}\mathbf{W}$ captures the combined effect of both the channel matrix and the bit-to-symbol mapping matrix. We can see from (7) that the original QAM detection problem has been transformed into an equivalent BPSK-like detection model.

Adopting the nondecorrelated signal model of [14], (7) can be further reformulated as

$$\mathbf{y} = \mathbf{q}_l b_l + \sum_{k \neq l} \mathbf{q}_k b_k + \mathbf{n} \triangleq \mathbf{q}_l b_l + \mathbf{v}_l \tag{8}$$

where $\mathbf{q}_l$ denotes the lth column of $\mathbf{Q}$, and b_l is the lth bit of $\mathbf{b}$, whereas $\mathbf{v}_l$ is the interference and noise term contaminating bit b_l, $l, k = 1, 2, \ldots, M_cN_T$.

For each bit b_l, we define an two-element bit probability vector $\mathbf{P}(l)$, whose mth element $P_m(b_l|\mathbf{y})$ is the current estimate of the *a posteriori* probability that $b_l = a_m$, where $m = 1, 2$, and $a_1 = +1$, $a_2 = -1$. The key idea of the PDA algorithm [11] is to approximate the interference plus noise term $\mathbf{v}_l$ as an N_R-variate colored Gaussian distributed random variable with a mean of

$$\mu_l = \sum_{k \neq l} \bar{b}_k \mathbf{q}_k \tag{9}$$

covariance of

$$\mathbf{V}_l = \sum_{k \neq l} \mathbf{V}_{b_k} \mathbf{q}_k \mathbf{q}_k^H + N_0 \mathbf{I} \tag{10}$$

and pseudocovariance [18] of

$$\mathbf{U}_l = \sum_{k \neq l} \mathbf{U}_{b_k} \mathbf{q}_k \mathbf{q}_k^T \tag{11}$$

where

$$\bar{b}_k = \sum_{m=1}^{2} a_m P_m(b_k|\mathbf{y}) \tag{12}$$

$$\mathbf{V}_{b_k} = \sum_{m=1}^{2} (a_m - \bar{b}_k)(a_m - \bar{b}_k)^* P_m(b_k|\mathbf{y}) \tag{13}$$

$$\mathbf{U}_{b_k} = \sum_{m=1}^{2} (a_m - \bar{b}_k)(a_m - \bar{b}_k)^T P_m(b_k|\mathbf{y}). \tag{14}$$

Here, $P_m(b_k|\mathbf{y})$ is initialized as a uniform distribution and will be replaced with an updated bit-probability at each iteration of the B-PDA detector.

Let

$$\mathbf{w} = \mathbf{y} - b_l \mathbf{q}_l - \sum_{k \neq l} \bar{b}_k \mathbf{q}_k \tag{15}$$

$$\varphi_m(b_l) \triangleq \exp\left(- \begin{pmatrix} \Re(\mathbf{w}) \\ \Im(\mathbf{w}) \end{pmatrix}^T \mathbf{\Lambda}_l \begin{pmatrix} \Re(\mathbf{w}) \\ \Im(\mathbf{w}) \end{pmatrix} \right) \tag{16}$$

where we have

$$\mathbf{\Lambda}_l \triangleq \begin{pmatrix} \Re(\mathbf{V}_l + \mathbf{U}_l) & -\Im(\mathbf{V}_l - \mathbf{U}_l) \\ \Im(\mathbf{V}_l + \mathbf{U}_l) & \Re(\mathbf{V}_l - \mathbf{U}_l) \end{pmatrix}^{-1} \tag{17}$$

while $\Re(\cdot)$ and $\Im(\cdot)$ represent the real and imaginary parts of a complex variable, respectively.

Since it is assumed that all the transmitted bits have equal *a priori* probabilities, the *a posteriori* bit probability is given as

$$\begin{aligned} P_m(b_l|\mathbf{y}) &= \frac{p_m(\mathbf{y}|b_l) P(b_l = a_m)}{\sum_{m=1}^{2} p_m(\mathbf{y}|b_l) P(b_l = a_m)} \\ &\approx \frac{\varphi_m(b_l)}{\sum_{m=1}^{2} \varphi_m(b_l)}. \end{aligned} \tag{18}$$

In summary, the algorithm proceeds as follows.

1) Initialization: Set the initial values of the bit probabilities $P_m(b_l|\mathbf{y})$ using a uniform distribution for $\forall l = 1, 2, \ldots, M_c N_T$ $\forall m = 1, 2$, i.e., $P_m(b_l|\mathbf{y}) = 0.5$. Set the iteration counter to $z = 1$.
2) Set the bit index to $l = 1$.
3) Based on the current values of $\{\mathbf{P}(k)\}_{k \neq l}$, compute $P_m(b_l|\mathbf{y})$ using (9)–(18), which will replace the value of the corresponding element of $\mathbf{P}(l)$.
4) If $l < M_c N_T$, let $l = l + 1$, and go to step 3). Otherwise, go to step 5).
5) If $\mathbf{P}(l)$ has converged $\forall l$ or the iteration index has reached its maximum, go to step 6). Otherwise, let $z = z + 1$, and return to step 2).
6) For $l = 1, 2, \ldots, M_c N_T$, make a decision concerning $\hat{b}_l$ using $\hat{b}_l = a_d$, $d = \arg\max_{m'=1,2}\{P_{m'}(b_l|\mathbf{y})\}$, yielding $\hat{\mathbf{b}} = \{\hat{b}_l | l = 1, 2, \ldots, M_c N_T\}$.

B. Discussions

From the preceding procedures, we can see that the size of the detected vector is extended from N_T symbols to $M_c N_T$ bits, and the number of constellation points is reduced from $M \geq 4$ to 2. It was demonstrated in [14] that the quality of "Gaussian approximation" and, therefore, of the soft outputs, is the best for a large number of transmit antennas and a small number of constellation points [14]. In this context, the question arises as to how the UMR of QAM will influence the achievable performance of the proposed B-PDA. This may not be an easy dilemma to resolve since the theoretical performance bound of PDA-based algorithms is still an open problem, and the UMR transformation may have both a positive and a negative impact on the achievable performance. First, based on the observations in [14], we intuitively infer that *our approach may be interpreted as virtually increasing the number of transmit antennas while reducing the QAM constellation to a binary constellation. This approach improves the quality of the Gaussian approximation and reduces the decision ambiguity concerning the symbols of high-order QAM since it leads to binary decisions.* Hence, the performance of B-PDA is expected to be enhanced. On the other hand, the UMR transformation may result into a degraded composite channel of $\mathbf{HW}$, which may deteriorate the achievable performance of B-PDA. We will demonstrate that, in fact, the composite effect of the UMR is positive, as it will be evidenced in Section VI.

To elaborate a little further, the design and choice of constellation labeling may have a significant impact on the BER performance of symbol-based detectors. This explains why our research community has been keen on investigating various labeling schemes in the context of different communication systems. However, the specific bit assignment within a symbol does not affect the SER performance, because the SER performance is determined by the minimum Euclidean distance of the constellation employed. However, since the proposed B-PDA skips the symbol-detection stage and directly operates at the bit level, where the bits are separately and independently treated, the correlation between bits may not affect the achievable BER performance, as seen from the simulation results in Section VI.

Note that, if Gray-mapping-based rectangular QAM is used in the preceding B-PDA-aided MIMO systems, it may be difficult to perfectly determine in advance the specific modulation matrix $\mathbf{W}(\mathbf{b})$ used at the receiver, because the modulation matrix depends on the transmitted bit vector. This implies that either a realistic detector should be used to first estimate the $\mathbf{W}(\mathbf{b})$ at the receiver or a flag containing the index of the modulation matrix used should be sent to the receiver via the signaling channel. Aside from the additional complexity, there would be a performance degradation, which is determined by the quality of the corresponding estimation algorithm. However, to provide a lower bound performance for the linear-natural-mapping-based B-PDA, we assume that the modulation

TABLE III
PROBABILITIES COMPUTED IN ONE ITERATION FOR CPDA

	1	2	$\cdots$	m	$\cdots$	M
$\mathbf{P}(1)$	$P_1(s_1\|\mathbf{y})$	$P_2(s_1\|\mathbf{y})$	$\cdots$	$P_m(s_1\|\mathbf{y})$	$\cdots$	$P_M(s_1\|\mathbf{y})$
$\mathbf{P}(2)$	$P_1(s_2\|\mathbf{y})$	$P_2(s_2\|\mathbf{y})$	$\cdots$	$P_m(s_2\|\mathbf{y})$	$\cdots$	$P_M(s_2\|\mathbf{y})$
$\vdots$	$\vdots$	$\vdots$	$\cdots$	$\vdots$	$\cdots$	$\vdots$
$\mathbf{P}(j)$	$P_1(s_j\|\mathbf{y})$	$P_2(s_j\|\mathbf{y})$	$\cdots$	$P_m(s_j\|\mathbf{y})$	$\cdots$	$P_M(s_j\|\mathbf{y})$
$\vdots$	$\vdots$	$\vdots$	$\cdots$	$\vdots$	$\cdots$	$\vdots$
$\mathbf{P}(N_T)$	$P_1(s_{N_T}\|\mathbf{y})$	$P_2(s_{N_T}\|\mathbf{y})$	$\cdots$	$P_m(s_{N_T}\|\mathbf{y})$	$\cdots$	$P_M(s_{N_T}\|\mathbf{y})$

matrix $\mathbf{W}(\mathbf{b})$ of the Gray-mapping scenario is perfectly known at the receiver in the simulations of Section VI. In fact, observe in Figs. 4–7 that the linear-natural-mapping-based B-PDA achieves almost the same performance as the Gray-mapping-based B-PDA under the idealized perfect modulation matrix estimation assumption.

C. Complexity Analysis

It was shown in [17] that the conventional symbol-based CPDA MIMO detector has to update an $(M \times N_T)$-element probability matrix at each iteration, until all the entries in the matrix converge or the maximum iteration index is reached. For the sake of clarity and compactness, this probability matrix is explicitly provided in the form of Table III. Consequently, the number of probabilities to be computed may be as high as MN_TN_{it} for each symbol vector $\mathbf{s}$, where N_{it} is the average number of iterations required for convergence in the process of detecting each M-QAM N_T-symbol vector.

By comparison, it may be readily observed from the aforementioned B-PDA procedures that, provided that the UMR of QAM is employed, the corresponding probability matrix for B-PDA has M_cN_T rows and two columns, as seen in Table IV. Thus, the number of probabilities to be computed reduces to $2M_cN_T$ at each iteration. Hence, the total number of probabilities to be computed becomes $2M_cN_TN'_{it}$, where N'_{it} is the average number of iterations required for detecting each corresponding bit vector. Additionally, the complexity imposed by computing a single probability is denoted as C_p and C'_p for CPDA and B-PDA, respectively.

Then, the achievable complexity ratio of the B-PDA MIMO detector over the conventional PDA MIMO detector required for decoding a single symbol vector becomes

$$R_c(M) = \frac{2M_cN_TN'_{it}C'_p}{MN_TN_{it}C_p} = \frac{2\log_2(M)}{M} \cdot \frac{N'_{it}}{N_{it}} \cdot \frac{C'_p(M)}{C_p(M)} \qquad (19)$$

where $2\log_2(M)C'_p(M)$ and $MC_p(M)$ are the per-iteration complexity for B-PDA and CPDA, respectively, whereas $2\log_2(M)N'_{it}C'_p(M)$ and $MN_{it}C_p(M)$ are the complexity per symbol vector for B-PDA and CPDA, respectively. Equation (19) is a monotonically decreasing function of the modulation order M, because the ratio of the number of iterations N'_{it}/N_{it} is typically close to 1, where $C'_p(M)/C_p(M)$ is less than 1 and decreases upon increasing M, as it will be demonstrated in Fig. 2.[5] Consequently, we have $R_c(M) \ll 1$ for $M \gg 4$. We provide a demonstrative example in Fig. 2 for the complexity comparison between the conventional CPDA and the proposed B-PDA quantified in terms of the number of FLoating point OPerations (FLOPs) per iteration and per symbol vector for different QAM constellations. It may be readily seen in Fig. 2 that the complexity of B-PDA using the linear natural bit mapping is reduced by about 80% for the system configuration of 64QAM, $N_T = N_R = 2$, and SNR $= 20$ dB.

TABLE IV
PROBABILITIES COMPUTED IN ONE ITERATION FOR B-PDA

	1	2
$\mathbf{P}(1)$	$P_1(b_1\|\mathbf{y})$	$P_2(b_1\|\mathbf{y})$
$\mathbf{P}(2)$	$P_1(b_2\|\mathbf{y})$	$P_2(b_2\|\mathbf{y})$
$\vdots$	$\vdots$	$\vdots$
$\mathbf{P}(l)$	$P_1(b_l\|\mathbf{y})$	$P_2(b_l\|\mathbf{y})$
$\vdots$	$\vdots$	$\vdots$
$\mathbf{P}(M_cN_T)$	$P_1(b_{M_cN_T}\|\mathbf{y})$	$P_2(b_{M_cN_T}\|\mathbf{y})$

VI. SIMULATION RESULTS

In this section, we characterize the achievable performance of the B-PDA algorithm using Monte Carlo (MC) simulations in the context of the VBLAST system [1] as a function of the average SNR per receive antenna (SNR $\triangleq 10\log_{10}(E\{\|\mathbf{Hs}\|^2/N_R\}/N_0) = 10\log_{10}(N_T/N_0)$) for transmission over flat Rayleigh fading channels, where the entries of the MIMO channel are independent and identically distributed (i.i.d.) zero-mean unit-variance complex-valued Gaussian random variables. A new independent channel realization is drawn for each transmitted symbol vector. The noise vector $\mathbf{n}$ is i.i.d. $\mathcal{CN}(0, N_0)$. No optimal ordering of the bits is performed before

[5]The average number of iterations of the conventional PDA MIMO detector is typically 3–5, as seen in [11] and [15], as well as in Figs. 2 and 3. In addition, the computational cost in terms of FLOPs for estimating the *a posteriori* probability of a BPSK-like signal is lower than that of a complex-valued multilevel QAM signal.

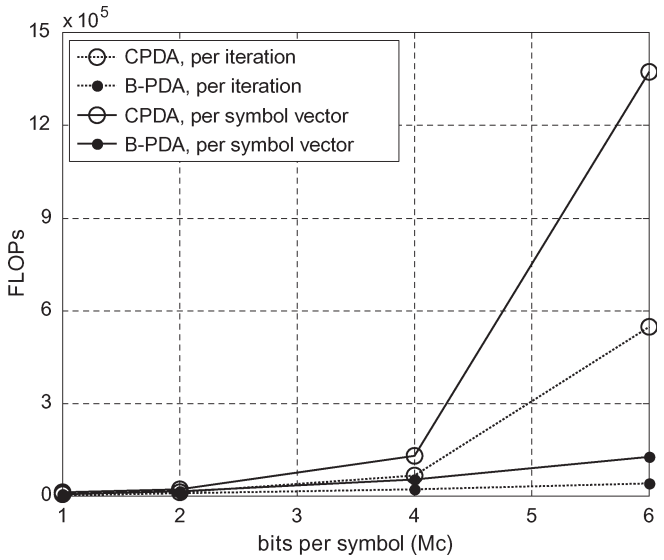

Fig. 2. Complexity comparison in FLOPs per iteration and per symbol vector for B-PDA with natural bit mapping and CPDA with Gray bit mapping using BPSK ($M_c = 1$), 4QAM ($M_c = 2$), 16QAM ($M_c = 4$), 64QAM ($M_c = 6$), SNR = 20 dB, and $N_T = N_R = 2$.

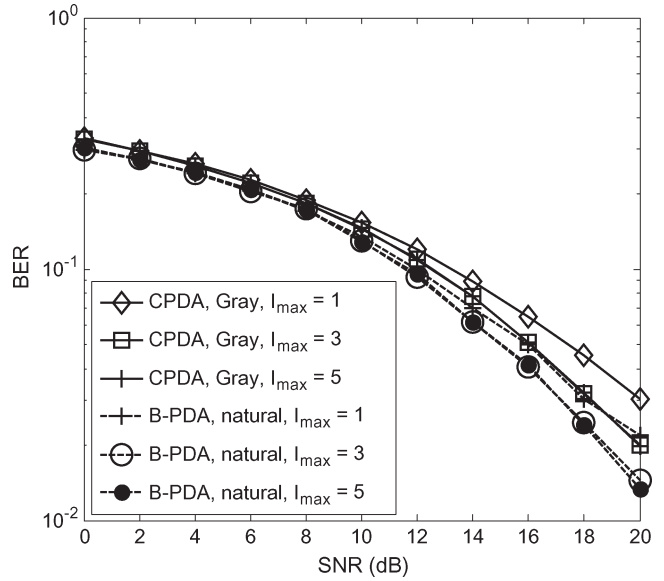

Fig. 3. Impact of the number of iterations on the achievable performance of CPDA and B-PDA in VBLAST using 16QAM ($N_T = N_R = 2$).

detection in the following PDA-related simulations for the sake of fair comparison with the results of [17]. The convergence threshold is set to $\varepsilon = |P_{i,j}^{z+1} - P_{i,j}^{z}| = 0.001$, where $P_{i,j}^{z}$ represents the (i,j)th value of the probability matrix of CPDA or B-PDA at the zth iteration.

To choose the appropriate number of iterations for the PDA-aided MIMO detectors, Fig. 3 evaluates the impact of the number of iterations on both the performance of the conventional symbol-based CPDA of [17] using Gray-mapping-based 16QAM and the proposed B-PDA using linear-natural-mapping-based 16QAM in the context of (2×2)-antenna aided VBLAST systems. The maximum number of iterations $I_{\max}$ is set to 1, 3, and 5, respectively. It can be seen from Fig. 3 that both the CPDA and B-PDA exhibit quite a good convergence

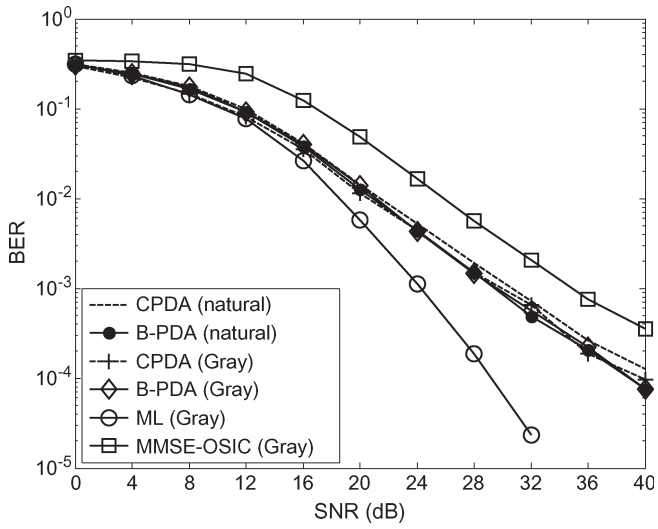

Fig. 4. BER Comparison of B-PDA and CPDA, MMSE-OSIC, and ML in VBLAST with 16QAM, $I_{\max} = 5$, and $N_T = N_R = 2$.

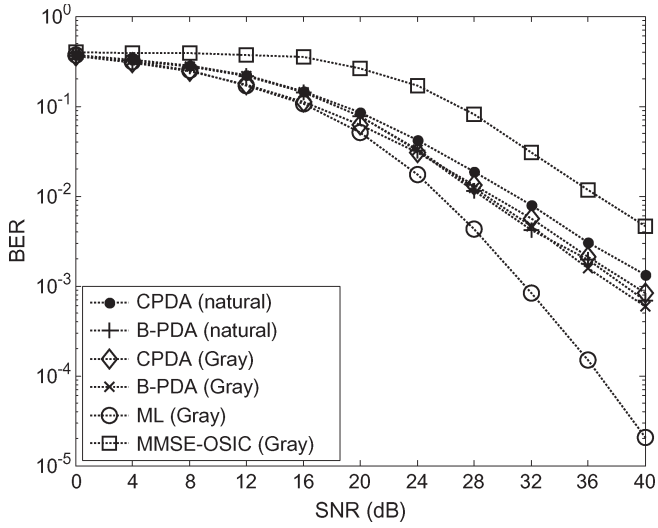

Fig. 5. BER Comparison of B-PDA and CPDA, MMSE-OSIC, and ML in VBLAST with 64QAM, $I_{\max} = 5$, and $N_T = N_R = 2$.

since the performance loss is modest, even when the maximum number of iterations is set to be as low as $I_{\max} = 3$.

Based on the preceding observation, we set the maximum number of iterations to $I_{\max} = 5$ in the following investigations, where B-PDA is compared with the conventional symbol-based CPDA, MMSE-ordered-SIC (MMSE-OSIC), and ML while using both the linear natural bit mapping and the nonlinear Gray mapping.[6] The pairs of Figs. 4–7 evaluate the attainable BER and SER performances, respectively, for both 16QAM and 64QAM constellations.[7] In general, the

[6]We treat the matrix $\mathbf{W}(\mathbf{b})$ as being perfectly known at the receiver, which is merely an idealized assumption for the nonlinear Gray-mapping-based B-PDA. Based on this assumption, the performance curve of the B-PDA plotted for the Gray-mapping scenario serves as a lower bound of the B-PDA performance in the linear natural mapping case.

[7]As pointed out in [22], for HOM, multiple bit errors occurring close to each other will probably create only one symbol error. In this situation, the SER is a useful metric that is widely adopted in the literature of the high-order M-ary detection in MIMO systems, as seen in [8], [10], and [15].

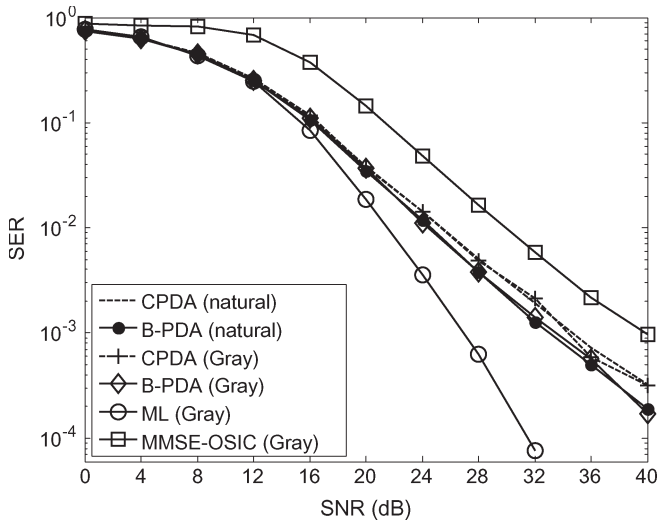

Fig. 6. SER Comparison of B-PDA and CPDA, MMSE-OSIC, and ML in VBLAST with 16QAM, $I_{\max} = 5$, and $N_T = N_R = 2$.

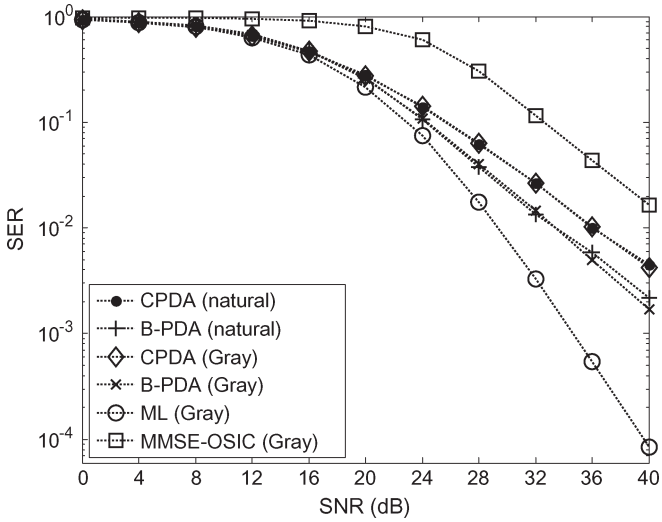

Fig. 7. SER Comparison of B-PDA and CPDA, MMSE-OSIC, and ML in VBLAST with 64QAM, $I_{\max} = 5$, and $N_T = N_R = 2$.

performance of B-PDA is superior to that of CPDA, and the attainable gain is more substantial in terms of SER. For the linear-natural-mapping-based 16QAM, B-PDA outperforms CPDA by approximately 2 dB at both BER $= 10^{-3}$ and SER $= 10^{-3}$. Similarly, for the linear-natural-bit-mapping-based 64QAM, the corresponding gains are up to 3 dB at BER $= 10^{-2}$ and SER $= 10^{-2}$. When the conventional symbol-based CPDA uses the nonlinear Gray mapping, it can be seen by comparing the results of Figs. 4 and 5 with those of Figs. 6 and 7 that the BER performance of the linear-natural-mapping-based B-PDA slightly erodes at low SNRs but still has an advantage over that of CPDA at high SNRs. Furthermore, observe from the SER curves of Figs. 6 and 7 that the SNR gain of the linear-natural-mapping-based B-PDA remains superior to that of CPDA at all the SNR values considered. This is *because Gray mapping is efficient in terms of reducing the BER through the binary labeling gain, but it is unable to improve the SER since the SER is determined by the minimum Euclidean distance of the constellation points (a single constellation may have various labeling schemes).*

It is also interesting to observe that the performance of the linear-natural-mapping-aided QAM approaches that of the Gray-mapping-aided QAM for the proposed B-PDA, whereas the latter represents a lower bound performance valid under the assumption of perfect knowledge of $\mathbf{W}(\mathbf{b})$ at the receiver. In other words, *B-PDA is insensitive to the specific choice between the nonlinear binary reflected Gray mapping and the linear natural mapping considered, as long as the matrix* $\mathbf{W}$ *or* $\mathbf{W}(\mathbf{b})$ *is known at the receiver. This is because it directly operates on the basis of the separate bits, i.e., in a bit-by-bit fashion, which independently treats each bit and remains unaffected by the specific correlation between the bits within a symbol.* By comparison, the conventional PDA generally makes the decision at the symbol level using the estimated *a posteriori* symbol probabilities, and if necessary, the bits are recovered according to the inverse bit-to-symbol mapping, which retains the better BER of Gray mapping but has no advantage in SER. Therefore, it may be concluded that it is not necessary to design complex bit-to-symbol mapping rules for the proposed B-PDA, because it is capable of approaching the lower bound performance provided by the Gray-mapping-based B-PDA in ideal conditions, even upon using the simplest linear natural bit-to-symbol mapping.

It can also be seen from Figs. 4–7 that the linear-natural-mapping-based B-PDA significantly outperforms MMSE-OSIC but remains inferior in comparison to the ML detector. This indicates that the proposed B-PDA may not be able to achieve the full diversity in the specific context considered.[8] To the best our knowledge, the theoretical performance analysis and the diversity order analysis of the PDA algorithm in the MIMO detection context still remain open questions. The challenge is that it proceeds in an iterative fashion, and the accuracy of approximating a multimodal Gaussian mixture probability structure with the aid of a single multivariate Gaussian distribution in PDA-based detectors may not always guarantee that the global optimum is achieved. We will investigate this issue in our future research.

VII. Conclusion

We have proposed a unified B-PDA detection scheme for spatial-multiplexing-based VBLAST-style MIMO systems. Based on the UMR of rectangular QAM, the B-PDA transforms the symbol detection process of QAM to that of a BPSK-like scenario with the aid of a composite channel matrix combining the effect of modulation and of the original channel matrix. Simulations and complexity analysis have demonstrated that the proposed B-PDA typically outperforms the conventional CPDA, despite its dramatically reduced complexity, particularly in the context of high-order QAM constellations. In

[8]Some other reduced-complexity MIMO detectors, such as, for example, the fixed-complexity sphere decoder and the SDR detector derived for binary signaling have been shown to be capable of achieving the full diversity [23], [24] under certain conditions, whereas the partial equalization approach of [25] achieves a diversity order between that of the ML and ZF solutions.

addition, the simulation results have shown that the linear-natural-mapping-based B-PDA is insensitive to the specific choice of the linear natural and the binary-reflected Gray labeling schemes considered and approaches the best-case performance provided by the Gray-mapping-based B-PDA with perfect modulation matrix assumption. Finally, we have concluded that it is preferable to use the simpler and more practicable linear natural bit-to-symbol mapping rather than Gray mapping for the B-PDA-aided MIMO detector in the uncoded VBLAST-style systems considered.

REFERENCES

[1] P. W. Wolniansky, G. J. Foschini, G. D. Golden, and R. A. Valenzuela, "V-BLAST: An architecture for realizing very high data rates over the rich-scattering wireless channel," in *Proc. URSI ISSSE*, Pisa, Italy, Sep. 1998, pp. 295–300.

[2] S. Verdu, *Multiuser Detection*. Cambridge, U.K.: Cambridge Univ. Press, 1998.

[3] E. Viterbo and J. Boutros, "A universal lattice code decoder for fading channels," *IEEE Trans. Inf. Theory*, vol. 45, no. 5, pp. 1639–1642, Jul. 1999.

[4] J. Jaldén and B. Ottersten, "On the complexity of sphere decoding in digital communications," *IEEE Trans. Signal Process.*, vol. 53, no. 4, pp. 1474–1484, Apr. 2005.

[5] E. G. Larsson, "MIMO detection methods: How they work [lecture notes]," *IEEE Signal Process. Mag.*, vol. 26, no. 3, pp. 91–95, May 2009.

[6] L. Hanzo, L.-L. Yang, E.-L. Kuan, and K. Yen, *Single and Multi-Carrier DS-CDMA: Multi-User Detection, Space-Time Spreading, Synchronisation, Networking and Standards*. Chichester, U.K.: Wiley-IEEE Press, 2003.

[7] X. Zhao and M. Davies, "A feasible blind equalization scheme in large constellation MIMO systems," in *Proc. IEEE ICASSP*, Las Vegas, NV, Mar. 31–Apr. 4, 2008, pp. 1845–1848.

[8] Z. Mao, X. Wang, and X. Wang, "Semidefinite programming relaxation approach for multiuser detection of QAM signals," *IEEE Trans. Wireless Commun.*, vol. 6, no. 12, pp. 4275–4279, Dec. 2007.

[9] Z. Luo, W. Ma, A. So, Y. Ye, and S. Zhang, "Semidefinite relaxation of quadratic optimization problems," *IEEE Signal Process. Mag.*, vol. 27, no. 3, pp. 20–34, May 2010.

[10] A. Mobasher, M. Taherzadeh, R. Sotirov, and A. K. Khandani, "A near-maximum-likelihood decoding algorithm for MIMO systems based on semi-definite programming," *IEEE Trans. Inf. Theory*, vol. 53, no. 11, pp. 3869–3886, Nov. 2007.

[11] J. Luo, K. R. Pattipati, P. K. Willett, and F. Hasegawa, "Near optimal multiuser detection in synchronous CDMA using probabilistic data association," *IEEE Commun. Lett.*, vol. 5, no. 9, pp. 361–363, Sep. 2001.

[12] Y. Bar-Shalom and X. R. Li, *Estimation and Tracking: Principles, Techniques and Software*. Dedham, MA: Artech House, 1993.

[13] D. Pham, J. Luo, K. Pattipati, and P. Willett, "A PDA-Kalman approach to multiuser detection in asynchronous CDMA," *IEEE Commun. Lett.*, vol. 6, no. 11, pp. 475–477, Nov. 2002.

[14] J. Fricke, M. Sandell, J. Mietzner, and P. Hoeher, "Impact of the Gaussian approximation on the performance of the probabilistic data association MIMO decoder," *EURASIP J. Wireless Commun. Netw.*, vol. 5, no. 5, pp. 796–800, Oct. 2005.

[15] D. Pham, K. Pattipati, P. Willet, and J. Luo, "A generalized probabilistic data association detector for multiple antenna systems," *IEEE Commun. Lett.*, vol. 8, no. 4, pp. 205–207, Apr. 2004.

[16] S. Liu and Z. Tian, "Near-optimum soft decision equalization for frequency selective MIMO channels," *IEEE Trans. Signal Process.*, vol. 52, no. 3, pp. 721–733, Mar. 2004.

[17] Y. Jia, C. M. Vithanage, C. Andrieu, and R. J. Piechocki, "Probabilistic data association for symbol detection in MIMO systems," *Electron. Lett.*, vol. 42, no. 1, pp. 38–40, Jan. 2006.

[18] F. D. Neeser and J. L. Massey, "Proper complex random processes with applications to information theory," *IEEE Trans. Inf. Theory*, vol. 39, no. 4, pp. 1293–1302, Jul. 1993.

[19] L. Hanzo, S. X. Ng, T. Keller, and W. Webb, *Quadrature Amplitude Modulation: From Basics to Adaptive Trellis-Coded, Turbo-Equalised and Space-Time Coded OFDM, CDMA and MC-CDMA Systems*, 2nd ed. Chichester, U.K.: Wiley-IEEE Press, 2004.

[20] T. Matsumoto, S. Ibi, S. Sampei, and R. Thoma, "Adaptive transmission with single-carrier multilevel BICM," *Proc. IEEE*, vol. 95, no. 12, pp. 2354–2367, Dec. 2007.

[21] E. Agrell, J. Lassing, E. Ström, and T. Ottosson, "On the optimality of the binary reflected Gray code," *IEEE Trans. Inf. Theory*, vol. 50, no. 12, pp. 3170–3182, Dec. 2004.

[22] J. Waschura, "C213: Bit error analysis and beyond," in *Proc. Commun. Des. Eng. Conf.*, Mar. 2000.

[23] J. Jaldén, L. G. Barbero, B. Ottersten, and J. S. Thompson, "Full diversity detection in MIMO systems with a fixed-complexity sphere decoder," in *Proc. IEEE ICASSP*, Honolulu, HI, Apr. 2007, vol. 3, pp. III-49–III-52.

[24] J. Jaldén and B. Ottersten, "The diversity order of the semidefinite relaxation detector," *IEEE Trans. Inf. Theory*, vol. 54, no. 4, pp. 1406–1422, Apr. 2008.

[25] J. Maurer, G. Matz, and D. Seethaler, "On the diversity-complexity tradeoff in MIMO spatial multiplexing systems," in *Proc. 40th ACSSC*, Pacific Grove, CA, Oct. 2006, pp. 2077–2081.

Shaoshi Yang (S'11) received the B.Eng. degree in information engineering from Beijing University of Posts and Telecommunications, Beijing, China, in 2006, respectively. He is currently working toward the Ph.D. degree in wireless communications under the support of the scholarships from both the University of Southampton and the China Scholarship Council with the School of Electronics and Computer Science, University of Southampton, Southampton, U.K.

His research interests include multiuser detection/multiple-input–multiple-output detection, multicell joint/distributed processing, and interference management.

Tiejun Lv (M'08) received the M.S. and Ph.D. degrees in electronic engineering from the University of Electronic Science and Technology of China, Chengdu, China, in 1997 and 2000, respectively.

From January 2001 to December 2002, he was a Postdoctoral Fellow with Tsinghua University, Beijing, China. From September 2008 to March 2009, he was a Visiting Professor with the Department of Electrical Engineering, Stanford University, Stanford, CA. He is currently a Professor with the Key Laboratory of Universal Wireless Communications, Beijing University of Posts and Telecommunications. He has published a number of technical papers on the physical layer of wireless mobile communications.

Dr. Lv is a Senior Member of the Chinese Electronics Association. He was the recipient of the "Program for New Century Excellent Talents in University" Award from the Ministry of Education, China, in 2006.

Robert G. Maunder (M'03) received the B.Eng. degree (first-class honors) in electronic engineering and the Ph.D. degree in wireless communications from the University of Southampton, Southampton, U.K., in 2003 and 2007, respectively.

He was also the recipient of a lectureship with the University of Southampton, where he is currently with the School of Electronics and Computer Science. His research interests include video coding, joint source/channel coding, and iterative decoding, on which he has published a number of IEEE papers.

Lajos Hanzo (F'04) received the B.S. degree in electronics in 1976, the D.Sc. degree in 1983, and the honorary doctorate *Doctor Honaris Causa* degree in 2009.

During his 34-year career in telecommunications, he has held various research and academic posts in Hungary, Germany, and the U.K. Since 1986, he has been with the School of Electronics and Computer Science, University of Southampton, Southampton, U.K., where he is the Chair in Telecommunications. He is also a Professorial Chair at Tsinghua University, Beijing, China. He has been a coauthor of 20 John Wiley-IEEE Press books on mobile radio communications, totaling more than 10 000 pages. He currently directs an academic research team, working on a range of research projects in wireless multimedia communications sponsored by industry, the Engineering and Physical Sciences Research Council, U.K., the European IST Program, and the Mobile Virtual Centre of Excellence, U.K. He is an enthusiastic supporter of industrial and academic liaison and offers a range of industrial courses. For further information on his research in progress and associated publications, see http://www-mobile.ecs.soton.ac.uk.

Dr. Hanzo is a Fellow of the Royal Academy of Engineering and the Institution of Engineering and Technology. He is also the Governor of the IEEE Communications Society and the IEEE Vehicular Technology Society. He is the Editor-in-Chief of the IEEE Press, has published about 970 research entries on IEEEXplore, acted as the Technical Program Committee Chair of IEEE conferences, presented keynote lectures, and received a number of distinctions.